Osteoprotegerin Diminishes Advanced Bone Cancer Pain

Nancy M. Luger, Prisca Honore, Mary Ann C. Sabino, et al.

Cancer Res 2001;61:4038-4047.

[CANCER RESEARCH 61, 4038–4047, May 15, 2001]

Osteoprotegerin Diminishes Advanced Bone Cancer Pain[1]

Nancy M. Luger, Prisca Honore,[2] Mary Ann C. Sabino, Matthew J. Schwei, Scott D. Rogers, David B. Mach, Denis R. Clohisy, and Patrick W. Mantyh[3]

Neurosystems Center and Departments of Preventive Sciences, Psychiatry, and Neuroscience [N. M. L., P. H., M. C. S., M. J. S., S. D. R., D. B. M., P. W. M.], Department of Orthopedic Surgery [D. R. C.], and Cancer Center [N. M. L., P. H., M. C. S., M. J. S., S. D. R., D. B. M., D. R. C., P. W. M.], University of Minnesota, Minneapolis, Minnesota 55455, and VA Medical Center, Minneapolis, Minnesota 55417 [N. M. L., P. H., M. C. S., M. J. S., S. D. R., D. B. M., P. W. M.]

ABSTRACT

Bone cancer pain most commonly occurs when tumors originating in breast, prostate, or lung metastasize to long bones, spinal vertebrae, and/or pelvis. Primary and metastatic cancers involving bone account for approximately 400,000 new cancer cases per year in the United States alone, and >70% of patients with advanced breast or prostate cancer have skeletal metastases. Whereas pain resulting from bone cancer can dramatically impact an individual's quality of life, very little is known about the mechanisms that generate and maintain this pain. To begin to define the mechanisms that give rise to advanced bone cancer pain, osteolytic 2472 sarcoma cells or media were injected into the intramedullary space of the femur of C3H/HeJ mice, and the injection hole was sealed using dental amalgam, confining the tumor cells to the bone. Twelve days after injection of 2472 tumor cells, animals showed advanced tumor-induced bone destruction of the injected femur, bone cancer pain, and a stereotypic set of neurochemical changes in the spinal cord dorsal horn that receives sensory inputs from the affected femur. Administration of osteoprotegerin, a naturally secreted decoy receptor that inhibits osteoclast maturation and activity and induces osteoclast apoptosis, or vehicle was begun at 12 days, when significant bone destruction had already occurred, and administration was continued daily until day 21. Ongoing pain behaviors, movement-evoked pain behaviors, and bone destruction were assessed on days 10, 12, 14, 17, and 21. The neurochemistry of the spinal cord was evaluated at days 12 and 21. Results indicated that osteoprotegerin treatment halted further bone destruction, reduced ongoing and movement-evoked pain, and reversed several aspects of the neurochemical reorganization of the spinal cord. Thus, even in advanced stages of bone cancer, ongoing osteoclast activity appears to be involved in the generation and maintenance of ongoing and movement-evoked pain. Blockade of ongoing osteoclast activity appears to have the potential to reduce bone cancer pain in patients with advanced tumor-induced bone destruction.

INTRODUCTION

Bone cancer occurs in patients with primary bone tumors (sarcomas and hematopoietic malignancies) and more commonly in patients with bone cancers that have metastasized from distant sites such as breast, prostate, or lung. Pain is the most frequent symptom of cancer-induced bone destruction. Bone metastases can significantly compromise the patient's quality of life because they induce bone fractures, hypercalcemia, neurologic deficits, and chronic pain (1–5).

While there is significant patient-to-patient variability in the severity and extent of bone cancer pain, there are generally two major components to bone cancer pain. The first component of bone cancer pain is described as a dull ache or throbbing in character and is frequently the first indication of tumor metastasis to a bone (3, 5). This initial pain is usually ongoing and increases in severity over time. A second component of bone cancer pain frequently emerges over time and is more acute in nature. This second type of pain is known as breakthrough or incident pain because it often occurs either spontaneously, with intermittent exacerbations of pain, or by movement of the cancerous bone (6–8). Commonly, breakthrough pain intensifies near the end of a dosing interval of scheduled analgesics. This breakthrough or incident pain represents one of the most serious and highly debilitating sequelae of cancer and is one of the most difficult cancer pains to treat (7, 8).

Currently, the treatment of bone cancer pain involves the use of a variety of different but complementary approaches including radiotherapy, analgesics, bisphosphonates, and surgery (3, 9–11). A major reason bone cancer pain is difficult to control is that bone metastases are generally not limited to a single site but are often present in multiple sites including the long bones, pelvis, and spinal vertebrae. Although radiotherapy remains the cornerstone for the treatment of bone cancer pain, it is most effective for the symptomatic treatment of local bone pain. When tumor cells have metastasized to multiple bones of the body, regional radiotherapy may be used. However, this treatment is accompanied by significant side effects such as vomiting, diarrhea, severe bone marrow depression, and acute pneumonitis secondary to alveolar cell damage (12, 13). Analgesics such as nonsteroidal anti-inflammatory drugs and opiates are also effective in treating bone cancer pain, but increasing doses are usually required as the cancer progresses. Additionally, complete control of breakthrough or movement-evoked pain can be problematic because the doses required to totally control this pain are usually high and are accompanied by adverse side effects such as cognitive impairment, sedation, and constipation (14).

In recent years, it has become clear that osteoclasts, the body's principal bone-resorbing cell, are required for cancer-induced bone destruction (15). Whereas recent work suggests that cancer-induced bone pain may be linked to bone resorption, very little is known about the precise mechanism(s) involved in the generation and maintenance of bone cancer pain (16). Until recently, bone cancer pain was thought to result primarily from mechanical instability of the bone that resulted in mechanical deformation and ensuing excitation of primary afferent fibers innervating the periosteum (17). However, recent data have suggested that the mechanisms that generate bone cancer pain may be more complex and involve the release of pronociceptive compounds from tumor and inflammatory cells, nerve compression, and ongoing osteoclast activity (18–20).

In previous work, we developed a murine model of bone cancer pain and established that approximately 50% of the ongoing and movement-evoked pain was blocked with elimination of osteoclast activity at the first sign of bone destruction, while the tumor grew unabated (16). Although these results are encouraging, significant skeletal destruction is present in 2% of patients at the time of initial diagnosis of breast cancer and in 30% of patients with recurring breast cancer (21). In these patients, in whom significant and ongoing skeletal destruction is already present, a major question with signifi-

Received 2/5/01; accepted 3/19/01.

The costs of publication of this article were defrayed in part by the payment of page charges. This article must therefore be hereby marked *advertisement* in accordance with 18 U.S.C. Section 1734 solely to indicate this fact.

[1] This study was supported by NIH grants from the National Institute of Neurologic Disorders and Stoke (NS23970) and the National Institute for Drug Abuse (11986), National Institute of Dental and Craniofacial Research Training Grant DE07288, National Institute of Arthritis and Musculoskeletal and Skin Diseases (AR43595), a Merit Review from the Veterans Administration, the Roby C. Thompson, Jr. Endowment in Musculoskeletal Oncology, a Dentist Scientist Award (DSA) DE00270, and a grant from the University of Minnesota Academic Health Center Strategic Initiative.

[2] Present address: Abbott Laboratories, Abbott Park, IL 60064.

[3] To whom requests for reprints should be addressed, at 18-208 Moos Towers, 515 Delaware Street, S.E., Minneapolis, MN 55455. Phone: (612) 626-0180; Fax: (612) 626-2565; E-mail: manty001@tc.umn.edu or clohi001@tc.umn.edu.

cant therapeutic implications is whether osteoclasts are still involved in generating and maintaining the bone cancer pain state. In the present report, we address this question using the murine model of bone cancer pain and eliminate the osteoclasts only when significant bone destruction has already occurred. Using simultaneous assessment of bone destruction, pain-related behaviors, and neurochemical changes in the spinal cord, we demonstrate that even when advanced cancer-induced bone destruction has occurred, halting osteoclast activity results in halting further bone destruction and reducing both ongoing and movement-evoked bone cancer pain.

MATERIALS AND METHODS

Bone Cancer Model. Experiments were performed on 44 adult male C3H/HeJ mice (Jackson Laboratories, Bar Harbor, ME) that were approximately 4–5 weeks old and weighed 20–25 g at the time of tumor cell injection. The mice were housed in accordance with NIH guidelines and kept in a vivarium maintained at 22°C with a 12-h alternating light/dark cycle, and they were given food and water *ad libitum*. All procedures were approved by the Animal Care and Use Committees of the University of Minnesota. Sarcoma injection protocol was performed as described previously (16). In brief, an arthrotomy was performed after administration of general anesthesia with sodium pentobarbital (50 mg/kg, i.p.). A needle was inserted into the medullary canal to create a pathway for the sarcoma cells. A depression was then made using a pneumatic dental high-speed handpiece. Sham animals ($n = 14$) were generated with an injection of α-MEM (20 μl; Sigma, St. Louis, MO) into the intramedullary space of the femur, whereas sarcoma-injected animals ($n = 22$) were injected with media containing 10^5 2472 osteolytic sarcoma cells (20 μl; American Type Culture Collection, Manassas, VA). For all animals, the injection site was sealed with a dental amalgam plug to confine the cells within the intramedullary canal, followed by irrigation with sterile water (hypotonic solution). Finally, incision closure was achieved with wound clips. Clips were removed at day 5 so as not to interfere with behavioral testing. Sham groups did not demonstrate significant differences in bone destruction or pain behaviors when compared with naïve C3H mice ($n = 8$).

Treatment with OPG.[4] A group of animals (sham 12 day, $n = 4$; sarcoma 12 day, $n = 5$) was used to assess the neurochemical state of the spinal cord in mice with advanced bone destruction. These mice did not receive any treatment. Initiation of OPG treatment on day 12 was selected because significant pain behaviors and bone destruction were observed at this time point. Animals were randomly divided into the following groups: (sham 21 day + vehicle, $n = 5$; sarcoma 21 day + vehicle, $n = 8$; sham 21 day + OPG, $n = 5$; sarcoma 21 day + OPG, $n = 9$). Beginning on day 12, sham and tumor groups received daily s.c. injections of either vehicle (Amgen, Thousand Oaks, CA; 50 μl) or vehicle containing OPG (Amgen; 5 mg/kg, 50 μl; Fig. 1). The OPG provided was a truncated form of human OPG containing amino acids 22–194 fused to the Fc domain of human IgG1 (22). OPG or vehicle treatment was terminated at 21 days postinjection of 2472 cells or media when final behavioral testing and euthanasia were performed.

Assessment of Bone Destruction. The extent of sarcoma-induced bone destruction (osteolysis) was assessed radiologically at a 4× magnification using Faxitron analysis (Specimen Radiography System Model MX-20; Faxitron X-ray Corp., Wheeling, IL; Kodak film Min-R 2000; Kodak, Rochester, NY). Faxitron images were taken before sarcoma or sham injections and at days 10, 12, 14, 17, and 21 after injection. Behavioral tests were also performed on the same days of Faxitron analysis to assess the relationship between the intensity of pain behaviors and bone destruction. Radiographs of tumor-bearing femora were scored on a previously validated scale of 0 to 5 (16). Using this scale, normal bone with no signs of destruction = 0, small pits of bone destruction (1–3 in number) = 1, increased pitted appearance (4–6 in number) and loss of medullary bone = 2, loss of medullary bone and erosion of cortical bone = 3, full thickness unicortical bone loss = 4, and full thickness bicortical bone loss and displaced skeletal fracture = 5.

[4] The abbreviations used are: OPG, osteoprotegerin; SPR, substance P receptor; GFAP, glial fibrillary acidic protein; IR, immunoreactive; DYN, dynorphin; RANK, receptor activator of nuclear factor κB; RANKL, RANK ligand; TNF, tumor necrosis factor; OPGL, OPG ligand; PLSD, protected least significant difference.

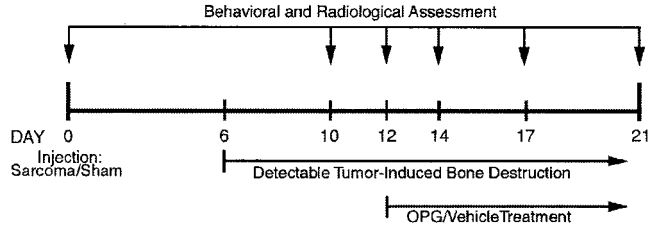

Fig. 1. Timeline and experimental outline. Behavioral testing was performed on days 0, 10, 12, 14, 17, and 21 (*arrows*). On day 12, when significant bone destruction had occurred, a group of sham and sarcoma-injected animals were sacrificed to assess bone destruction and the neurochemical state of the spinal cord after significant bone destruction had occurred (average bone score of 3 for sarcoma-injected animals). Vehicle or OPG (5 mg/kg) was administered daily from days 12–21 via s.c. injection. On day 21, the remaining groups of animals [sham + vehicle (days 12–21); sham + OPG (days 12–21); sarcoma + vehicle (days 12–21); and sarcoma + OPG (days 12–21)] were evaluated.

Behavioral Analysis. All mice were tested for pain-related behaviors before sarcoma or sham injections and then tested at days 10, 12, 14, 17, and 21 after injection. Ongoing and movement-evoked pain behaviors were analyzed as described previously (16). C3H/HeJ mice were allowed to habituate for a period of 30 min, and behavioral tests used to measure ongoing and movement-evoked pain were performed. Quantification of spontaneous flinches was used to measure ongoing pain. Limb use during normal ambulation in an open field, guarding during forced ambulation, and measurement of palpation-induced flinching after a 2-min period of normally non-noxious palpation of the distal femur were used as indications of movement-evoked pain. To monitor the general health of the animal, weights were recorded at each of the behavioral time points examined.

Euthanasia and Processing of Tissue. To determine the state of the spinal cord before vehicle or OPG treatment, sham and sarcoma animals were sacrificed at day 12, and their tissue was processed as described below. The remaining animals were sacrificed at day 21 and processed for radiological and immunohistochemical analysis. In addition, animals received a normally non-noxious palpation or mechanical stimulation of the tumor-bearing knee (every second for 2 min) 1.5 h and 5 min before euthanasia for visualization of c-Fos expression (23, 24) and substance P receptor internalization (25–27), respectively. After these manipulations, the animals were deeply anesthetized with sodium pentobarbital (50 mg/kg, i.p.) and perfused intracardially with 12 ml of 0.1 M PBS followed by 25 ml of 4% formaldehyde in 0.1 M PBS. Both ipsilateral and contralateral femora and spinal cord segments L1–S2 were removed, postfixed for 16 h in the perfusion fixative, and cryoprotected for 24 h in 30% sucrose in 0.1 M PBS (16, 28–31).

Immunohistochemistry. As described previously (16, 28–31), serial frozen coronal spinal cord sections were cut at 60 μm on a sliding microtome, collected in PBS, and processed as free-floating sections. The tissue sections were incubated for 30 min at room temperature in a blocking solution of 1% normal donkey serum in PBS with 0.3% Triton ×-100 followed by incubation overnight at room temperature in the primary antiserum, which is made in blocking solution. Markers of (*a*) spinal cord neurons [c-Fos protein (c-Fos; polyclonal rabbit anti-Fos; 1:20,000; Oncogene Research, San Diego, CA), DYN (polyclonal guinea pig antipreprodynorphin, 1:10,000, gift from Dr. R. Elde, University of Minnesota), and SPR (polyclonal rabbit anti-SPR, 1:5,000; raised in our laboratory); (*b*) and astrocytes [GFAP (polyclonal rabbit anti-GFAP, 1:600; Dako, Carpinteria, CA)] were used to immunostain spinal cord sections. After incubation, tissue sections were washed three times for 10 min each time in PBS and incubated in the secondary antibody solution for 2 h at room temperature. Secondary antibodies conjugated to the fluorescent marker cyanin 3, (Cy3; Jackson ImmunoResearch, West Grove, PA) were used at 1:600. Finally, the sections were washed three times for 10 min each time in PBS, mounted on gelatin-coated slides, air-dried, dehydrated via an alcohol gradient (70%, 90%, and 100%), cleared in xylene, and coverslipped using DPX (Fluka, Buchs, Switzerland). To confirm the specificity of the primary antibody, controls included preabsorption with the corresponding synthetic peptide or omission of the primary antibody. To control for the possibility that staining intensities might vary between experiments, control sections of normal C3H/HeJ mouse spinal cord were included in each run of staining and served as a standard for immunofluorescence measurements.

Quantification of Immunofluorescence Levels and SPR Internalization. Using an MRC-1024 Confocal Imaging System (Bio-Rad) and an Olympus BH-2 microscope equipped for epifluorescence, sections from the lumbar spinal cord were analyzed by conventional fluorescence and confocal microscopy to characterize immunofluorescence levels for GFAP expression, number of DYN- and c-Fos IR cells, and quantification of palpation-induced SPR internalization (16, 27, 30).

Quantification was performed in the spinal cord at lumbar level L4 because this spinal segment is one of the main projection sites of primary afferent fibers innervating the hindlimbs (32). Immunofluorescence intensity measurements were obtained using a 12-bit SPOT2 digital camera (Diagnostic Instruments Inc., Sterling Heights, MI) on an Olympus BX-60 fluorescence microscope with Image Pro Plus v.3.0 software (Media Cybernetics, Silver Spring, MD). The digital camera response was measured using 540/560 nm Inspeck fluorescent bead standards (Molecular Probes, Eugene, OR). A ratio was established between the output of the camera and a given relative fluorescence of the beads. The camera response was determined to be linear, thus establishing that a doubling of the camera grayscale output represents a doubling of label present in the tissue.

The number of c-Fos-IR neurons was counted in laminae I-II and V-VI, and the number of DYN-IR neurons was counted in laminae III-VI of the dorsal horn in 10 randomly selected L4 coronal sections/animal. Results are given as the mean number of c-Fos-IR or DYN-IR neurons/L4 section/group.

GFAP measurements were expressed as a percentage of contralateral as there was no difference in GFAP immunofluorescence in the contralateral side of the spinal cord of tumor-bearing mice as compared with naïve mouse spinal cord (16). The contralateral side of the mouse spinal cord served as an internal control for GFAP immunofluorescence for each experiment.

For quantification of SPR internalization, coronal sections were viewed through a 1 cm^2 eyepiece grid divided into one hundred 1 $\times$ 1-mm units. In cell bodies that have not internalized the SPR, SPR immunoreactivity is uniformly distributed on the cell surface. In contrast, in the neurons that have internalized the SPR, the cytoplasm contains bright SPR-IR endosomes. A SPR-IR endosome was defined as an intense SPR-IR intracellular organelle between 0.1 and 0.7 μm in diameter that was clearly not part of the external plasma membrane. In the present study, the number of SPR-IR endosomes/SPR-IR neuron was counted, and the results were expressed as the mean number of SPR-IR endosomes/internalized SPR-IR neuron in lamina I after normally non-noxious palpation. The current method of quantifying SPR internalization was selected due to difficulties that arose when coronal sections were used because there are a low number of neurons/coronal sections (16).

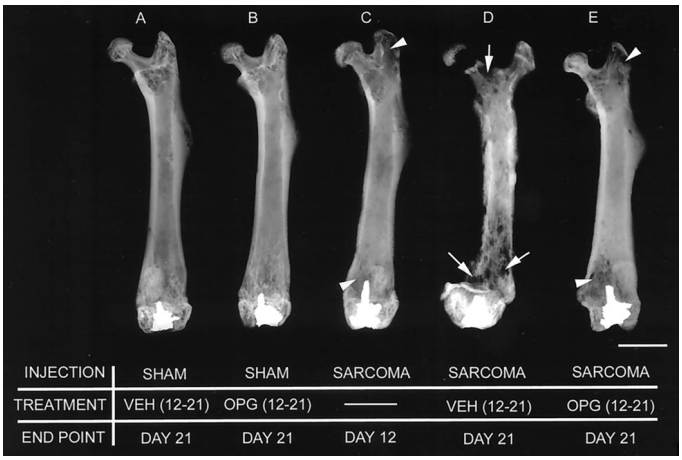

Fig. 2. High-resolution radiographs of mouse femurs demonstrate that OPG halts the progression of tumor-induced bone destruction. Sham-injected animals that received either vehicle (*A*) or OPG (*B*) from days 12–21 did not exhibit significant bone destruction or bone formation and therefore had a bone destruction score of 0. However, sarcoma-injected animals show advanced bone destruction before OPG treatment at day 12 (*C*; bone destruction score of 3) with pathological fractures frequently occurring by day 21 in vehicle-treated animals (*D*; bone destruction score of 5). Note the extreme bone destruction in sarcoma-injected animals that received vehicle (*D*, see the *white arrows*). In contrast, the bone destruction for sarcoma-injected mice that received OPG treatment (*E*, see the *white arrowheads*) remained the same and was not statistically different from that of sarcoma-injected mice at 12 days after tumor implantation. (*C*, see *white arrowheads*). *Scale bar*, 4 mm.

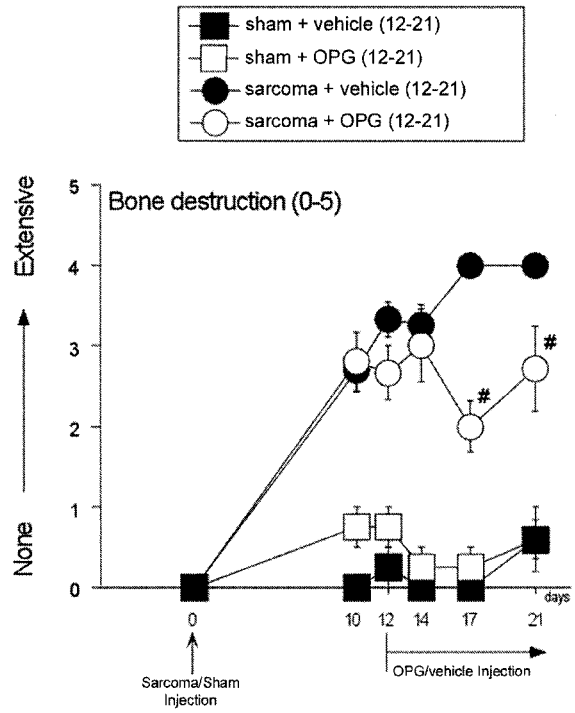

Fig. 3. Line graph showing that OPG rapidly halts tumor-induced bone destruction. Femurs from sham and sarcoma-injected animals that received either vehicle or OPG from day 12–21 (OPG, 5 mg/kg/day, s.c.) were assessed radiologically and scored. Advanced bone destruction was observed at day 12 after tumor implantation and progressed with time in vehicle-treated sarcoma-injected animals. However, OPG treatment arrested further bone destruction in sarcoma-injected animals, because bone destruction scores were not significantly different between pre- and post-OPG treatment sarcoma-injected groups. Results are expressed as the mean $\pm$ SEM. #, $P < 0.05$ as compared with sarcoma-injected vehicle-treated animals (one-way ANOVA, Fisher's PLSD).

Statistical Tests. A one-way ANOVA was used to compare bone destruction scores, behavioral results, and immunohistochemical measures (immunofluorescence levels and counts) between the experimental groups. For multiple comparisons, Fisher's PLSD *post hoc* test was used. Significance level was set at $P < 0.05$. The investigator responsible for scoring bone destruction, behavioral testing, and immunohistochemical quantification was blind to the experimental situation of each animal.

RESULTS

OPG Treatment Stops Tumor-induced Bone Destruction. Radiological bone destruction is first evident in the distal aspect of the femur 6 days after implantation of the lytic tumor cell line. As time and disease progress, the tumor spreads proximally. By 12 days after implantation, multiple focal radiolucencies are noted in both proximal and distal aspects of the femur. Radiographic analysis was used to measure the extent of tumor-induced bone destruction. The bone destruction scoring system assigned scores ranging from 0 (no bone destruction) to 5 (bicortical destruction and skeletal fracture). The mean bone score of day 12 sarcoma-injected femora was 2.7 $\pm$ 0.2. A significant increase in bone destruction score was observed in day 21 vehicle-treated sarcoma-injected animals (4.0 $\pm$ 0.0; $P < 0.05$ *versus* day 12 sarcoma-injected animals; Figs. 2 and 3). However, sarcoma-injected animals that received OPG treatment from day 12 to day 21 had a mean bone score of 2.7 $\pm$ 0.5 (not significantly different from day 12 sarcoma-injected animals; $P < 0.05$ *versus* day 21 sarcoma-injected animals receiving vehicle and respective sham animals). Therefore, OPG stabilized but did not reverse bone destruction because the bone scores of OPG-treated animals at day 21 remained the same as those at day 12 before OPG treatment.

OPG Treatment Stabilizes Bone Cancer-induced Pain-related Behaviors. OPG treatment reduced established cancer-induced skeletal pain. The number of spontaneous flinches during a 2-min period is a measurement of ongoing pain. Limb use, activity-related guarding, and palpation-evoked flinching behavior are measurements of movement-evoked pain. These pain behaviors mirror the clinical observation of breakthrough pain, which is experienced after movement of tumor-bearing limbs in bone cancer patients. All behaviors indicative of pain were stabilized after OPG treatment (Fig. 4).

Day 12 sarcoma-injected animals exhibited 10 ± 2 flinches ($P < 0.001$ *versus* respective sham), whereas day 21 vehicle-treated sarcoma-injected animals exhibited 11 ± 2 flinches (not different from day 12 animals; $P < 0.0001$ *versus* respective sham). OPG treatment significantly reduced the number of spontaneous flinches by 49% in day 21 OPG-treated sarcoma-injected animals (6 ± 1 flinches; $P < 0.01$ *versus* day 21 vehicle-treated sarcoma-injected animals; no statistical difference *versus* day 12 sarcoma-injected animals; $P < 0.002$ *versus* respective sham; Fig. 4*A*).

Limb use was reduced by 35 ± 4.5% in sarcoma-injected animals at day 12, pre-OPG treatment, as compared with sham animals ($P < 0.0001$). The reduction in limb use was even more pronounced at day 21 in vehicle-treated sarcoma-injected animals (54 ± 3.6% reduction; $P < 0.05$ *versus* day 12 sarcoma-treated animals; $P < 0.001$ *versus* sham animals). OPG-treated sarcoma-injected animals had a reduction in limb use comparable to day 12 sarcoma-injected animals (32 ± 7.2% reduction; $P < 0.05$ *versus* day 21 vehicle-treated sarcoma-injected animals; not different from day 12 sarcoma-injected animals; $P < 0.0001$ *versus* respective sham; Fig. 4*B*).

Similarly, OPG treatment stabilized activity-related guarding (Fig. 4*C*). Activity-related guarding mirrors the clinical observation of guarding of the tumor-bearing limb while bone cancer patients ambulate. At day 12, sarcoma-injected animals had a mean score of 2.3 ± 0.2 ($P < 0.001$ *versus* respective sham). The mean score at day 21 for vehicle-treated sarcoma-injected animals had increased to 3.3 ± 0.2 ($P < 0.05$ *versus* day 12 sarcoma-injected animals; $P < 0.005$ *versus* sham), whereas activity-related guarding in OPG-treated sarcoma-injected animals remained at 2.3 ± 0.4 ($P < 0.05$ *versus* day 21 sarcoma-injected animals receiving vehicle; not significantly different from day 12; $P < 0.001$ as compared with respective sham).

Additionally, OPG treatment in sarcoma-injected animals reduced palpation-evoked flinching induced by a normally non-noxious palpation. Day 12 sarcoma-injected animals exhibited 12.8 ± 1 palpation-induced flinches ($P < 0.0001$ *versus* sham). Day 21 vehicle-treated sarcoma-injected animals had 12.4 ± 2 palpation-induced flinches (not different from day 12 sarcoma-injected animals; $P < 0.005$ *versus* respective sham). OPG treatment reduced the number of palpation-induced flinches in OPG-treated sarcoma-injected animals (8.5 ± 0.7 palpation-induced flinches; $P < 0.05$ *versus* day 21 vehicle-treated sarcoma-injected animals, day 12 sarcoma-injected animals, and respective sham). These data show that both ongoing and movement-evoked pain behaviors are stabilized with OPG treatment.

OPG Treatment Alters Cancer-induced Neurochemical Reorganization of the Spinal Cord. To determine whether tumor implantation in the bone leads to an increased activity of primary afferent neurons, we counted the number of c-Fos-IR neurons in L4 spinal cord sections. Nociceptive or painful conditions have been associated with an increase in the number of c-Fos-IR neurons in the spinal cord (23, 26, 27, 33–37). Expression of the immediate early gene *c-fos* has been used as a marker of responses to cell surface stimulation, such as that seen with synaptic activity (38). Thus, c-Fos immunoreactivity is

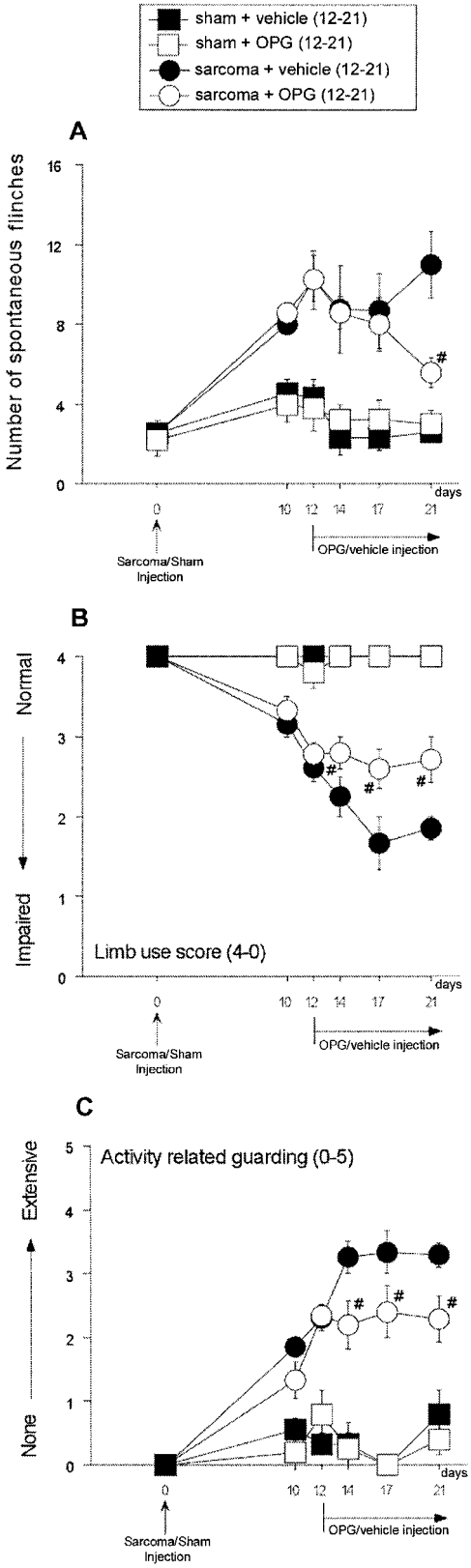

Fig. 4. Line graph showing that OPG treatment reduces both ongoing and movement-evoked pain-related behaviors in sarcoma-injected animals. Ongoing pain assessment includes the number of spontaneous flinches (*A*), whereas movement-evoked pain is measured by limb use score (*B*), and activity-related guarding (*C*) in sham and sarcoma-injected animals that received either vehicle or OPG from day 12–21 (OPG, 5 mg/kg/day, s.c.). Note that sarcoma-injected animals receiving OPG treatment had a significantly reduced number of spontaneous flinches. Moreover, OPG treatment stabilized limb use score and activity-related guarding in sarcoma-injected animals. Values represent the mean ± SEM. #, $P < 0.05$ as compared with sarcoma-injected vehicle-treated animals (one-way ANOVA, Fisher's PLSD).

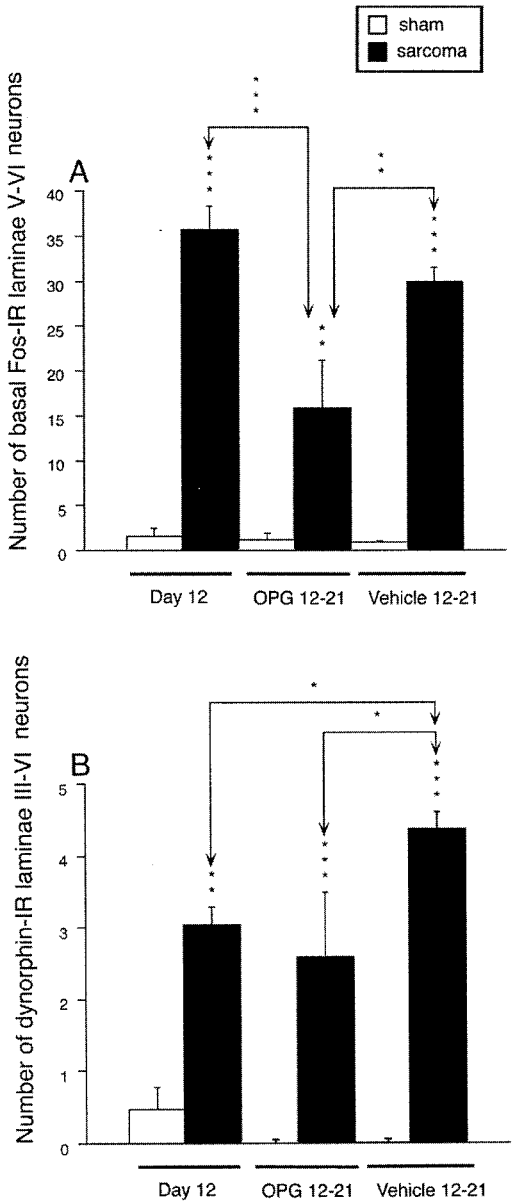

Fig. 5. Histogram showing that OPG treatment reduces basal c-Fos expression and stabilizes DYN expression in the spinal cord of sarcoma-injected animals. Results are expressed as the number of c-Fos-IR laminae V-VI spinal neurons/L4 section (*A*) and DYN-IR laminae III-VI spinal neurons/L4 section (*B*) in sham and day 12 sarcoma-injected animals before treatment and in day 21 animals after OPG or vehicle treatment. Values represent the mean ± SEM. One-way ANOVA, Fisher's PLSD: *, $P < 0.05$; **, $P < 0.01$; ***, $P < 0.001$ [as compared with respective sham animals (*brackets* and *downward arrows* indicate the groups being compared)].

a tool that has been widely used by neurobiologists to map mono- and multisynaptic pathways in the central nervous system (23, 39). At day 12, there was a significant increase in the number of c-Fos-IR laminae V-VI neurons ipsilateral to the sarcoma-injected femur (35.6 ± 2.6 neurons/L4 section) as compared with sham values (1.6 ± 1.0 neurons/L4 section; $P < 0.001$; Figs. 5*A* and 6). Day 21 vehicle-treated sarcoma-injected animals also showed an increase in c-Fos-IR neurons (30.0 ± 3.5 neurons/L4 section) as compared with sham values (0.9 ± 0.6 neurons/L4 section; $P < 0.001$; not different *versus* day 12 sarcoma-injected animals). However, OPG-treated sarcoma-injected animals had significantly fewer c-Fos-IR neurons at day 21 (15.8 ± 5.4 neurons/L4 section; $P < 0.01$ *versus* day 21 sarcoma-injected animals; $P < 0.05$ *versus* day 12 sarcoma-injected animals; $P < 0.01$ *versus* respective sham).

DYN is a prohyperalgesic peptide whose expression in the spinal cord has been implicated in chronic pain states (40, 41). OPG treatment stabilized the appearance of DYN-IR neurons in the spinal cord of sarcoma-injected animals (Figs. 5*B* and 7). Day 12 sarcoma-injected animals had a significant ipsilateral increase in the number of DYN-IR laminae III-VI neurons (3.0 ± 0.3 DYN-IR neurons/L4 section) compared with sham values (0.5 ± 0.3 DYN-IR neurons/L4 section; $P < 0.01$). Day 21 vehicle-treated sarcoma-injected animals had an ipsilateral increase in DYN-IR laminae III-VI neurons (4.4 ± 0.6 DYN-IR neurons/L4 section; $P < 0.05$ *versus* day 12 sarcoma-injected animals; $P < 0.001$ *versus* respective sham). The ipsilateral increase of DYN-IR III-VI neurons was stabilized in sarcoma-injected animals receiving OPG treatment (2.6 ± 0.9 DYN-IR neurons/L4 section) because the number of DYN-IR laminae III-VI neurons was not significantly different from that of day 12 sarcoma-injected animals but was different from than day 21 sarcoma-injected animals that received vehicle ($P < 0.05$) and respective sham (0.0 ± 0.0 DYN-IR neurons/L4 section; $P < 0.01$).

Astrocyte hypertrophy was observed in day 12 sarcoma-injected animals, day 21 vehicle-treated sarcoma-injected animals, and day 21 OPG-treated sarcoma-injected animals. At day 12, the sarcoma-injected mice had a significant ipsilateral increase in GFAP immunofluorescence (59.0 ± 1.9% increase in GFAP-IF/L4 section compared with respective sham; $P < 0.05$). Day 21 vehicle-treated sarcoma-injected animals had a 125.3 ± 3.9% increase in GFAP/L4 section ($P < 0.05$ *versus* respective sham), whereas OPG-treated sarcoma-

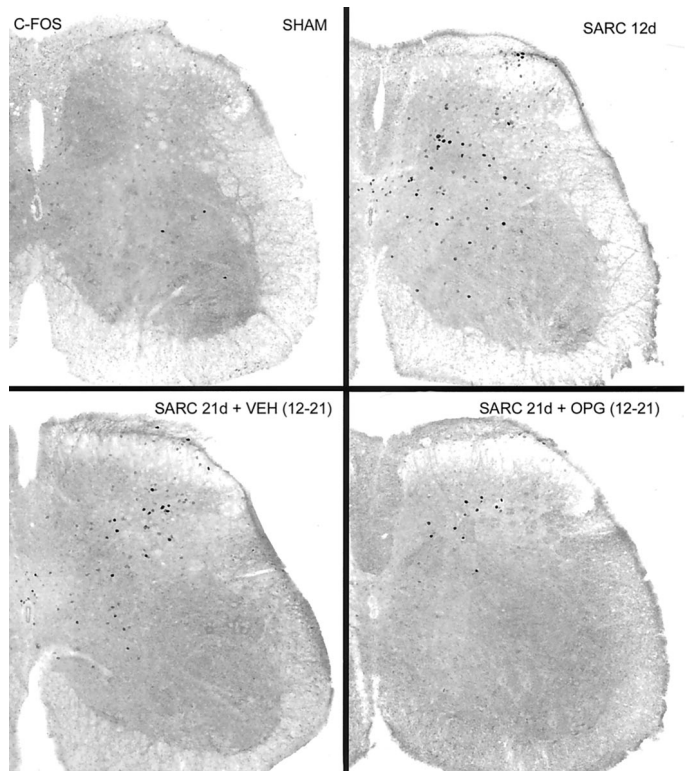

Fig. 6. Confocal images showing that the elimination of ongoing osteoclast activity reduces palpation-induced primary afferent sensitization. Confocal images of the spinal cord ipsilateral to tumor implantation demonstrate the distribution of c-Fos in coronal sections of the L4 spinal segment in sham-injected mice that received either vehicle or OPG (*A*), in sarcoma-injected mice at day 12 before treatment (*B*), in sarcoma-injected mice that received vehicle from day 12–21 (*C*), and in sarcoma-injected mice that received OPG treatment from day 12–21 (*D*). Note that OPG treatment from days 12–21 stabilized the expression of c-Fos immunoreactivity throughout the dorsal horn of the spinal cord in sarcoma-injected animals. Images were obtained from 60-μm-thick tissue sections and projected from 10 optical sections acquired at 5-μm intervals with a ×20 lens; *scale bar* = 200 μm.

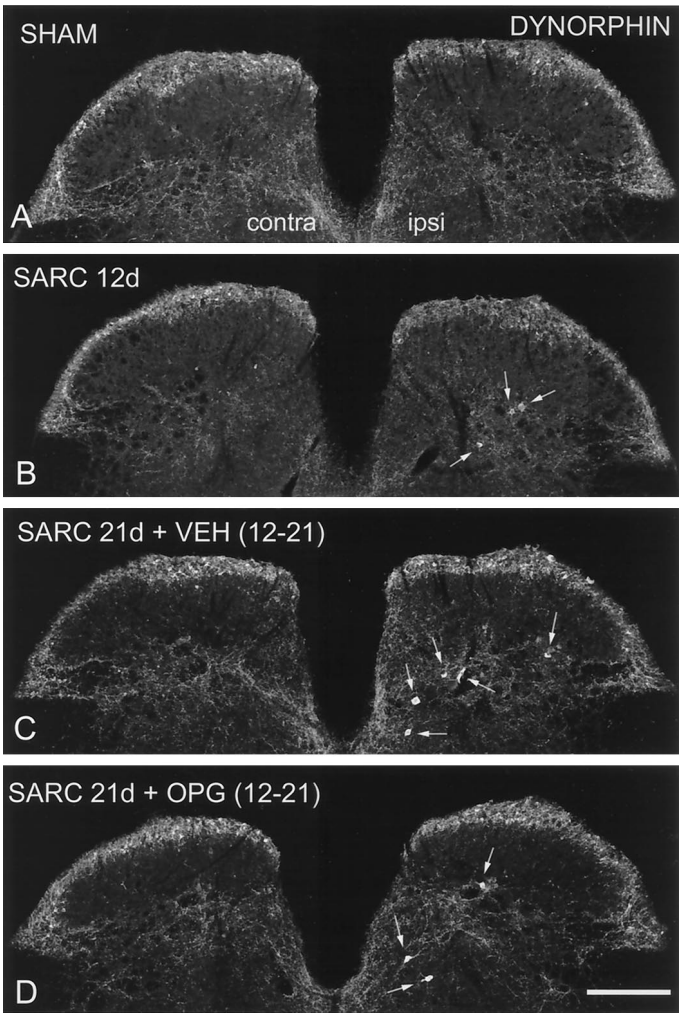

Fig. 7. Confocal images showing that elimination of ongoing osteoclast activity prevents a further increase of the prohyperalgesic peptide DYN in laminae III-VI of the spinal cord, ipsilateral to the sarcoma injection. Confocal images of the spinal cord demonstrate the distribution of DYN-IR neurons in coronal sections of the L4 spinal segment in sham-injected mice that received either vehicle or OPG (*A*), in sarcoma-injected mice at day 12 (*B*), in sarcoma-injected mice that received vehicle from days 12–21 (*C*), and in sarcoma-injected mice that received OPG treatment from days 12–21 (*D*). Note that vehicle-treated sarcoma-injected animals at day 21 (*C*) had increased DYN expression as compared with both sarcoma-injected animals at day 12 (*B*) and OPG-treated sarcoma-injected animals at day 21 (*D*). Images were obtained from 60-μm-thick tissue sections and projected from 10 optical sections acquired at 5-μm intervals with a $\times$20 lens; *scale bar* = 300 μm.

injected animals had a 154 $\pm$ 6.0% increase in GFAP immunofluorescence/L4 section ($P < 0.05$ *versus* respective sham). No differences were observed between day 12 sarcoma-injected animals, day 21 vehicle-treated sarcoma-injected animals, and day 21 OPG-treated sarcoma-injected animals.

OPG treatment reduces sensitization of primary afferent neurons observed after a normally non-noxious palpation of the affected limb. A normally non-noxious palpation did not induce c-Fos expression in laminae I-II in sham animals (1.5 $\pm$ 1.0 c-Fos-IR neurons/L4 section). However, in day 12 sarcoma-injected animals, an increase in the number of c-Fos-IR neurons in laminae I-II (9.5 $\pm$ 2.5 c-Fos-IR neurons/L4 section; $P < 0.001$ *versus* sham) was observed after normally non-noxious stimulation (Figs. 6 and 8*A*). An increase in c-Fos expression was also observed in day 21 vehicle-treated sarcoma-injected animals (9.8 $\pm$ 1.5 c-Fos-IR neurons/L4 section; not different from day 12 sarcoma-injected animals; $P < 0.001$ *versus* respective sham). OPG treatment in sarcoma-injected animals attenuated lamina I-II c-Fos expression (3.9 $\pm$ 1.5 c-Fos-IR neurons/L4 section; $P < 0.01$ *versus* day 21 sarcoma-injected vehicle-treated animals; $P < 0.05$ *versus* day 12 sarcoma-injected animals and not different from sham values).

OPG treatment eliminated the palpation-induced substance P release and subsequent SPR internalization observed in the spinal cord of sarcoma-injected animals (Fig. 8*B*). SPR immunoreactivity is distributed along the plasma membrane of SPR-expressing neurons in a normal non-stimulated animal. Sham animals did not show SPR internalization after a normally non-noxious palpation (0 $\pm$ 0 SPR-IR endosomes/L4 section). An average of 25.1 $\pm$ 6.3 SPR-IR endosomes were observed in SPR-IR lamina I neurons/L4 section of day 12 sarcoma-injected animals ($P < 0.001$ *versus* respective sham). An

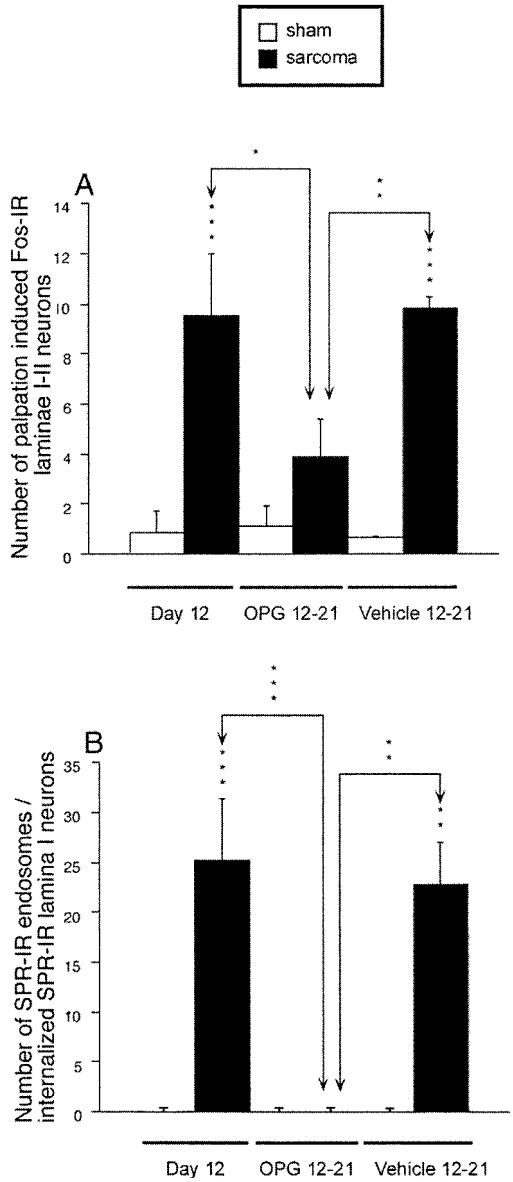

Fig. 8. Histogram showing that ongoing osteoclast activity is involved in the sensitization of primary afferent neurons in advanced bone cancer pain. Results are expressed as the mean number of c-Fos-expressing laminae I-II neurons (*A*) and the number of SPR-IR endosomes in lamina I SPR-IR neurons (*B*) after normally non-noxious palpation in sham and sarcoma-injected animals before OPG treatment and after OPG or vehicle treatment. Note that OPG treatment from day 12–21 abolishes spinal laminae I-II c-Fos expression and SPR internalization induced by a normally non-noxious palpation at day 21 in sarcoma-injected mice. One-way ANOVA, Fisher's PLSD: $*$, $P < 0.05$; $**$, $P < 0.01$; $***$, $P < 0.01$ [as compared with respective sham animals (*brackets* and *downward arrows* indicate the groups being compared)].

average of 22.8 ± 9.0 SPR-IR endosomes were observed in day 21 vehicle-treated sarcoma-injected animals (not different from day 12 sarcoma-injected animals; $P < 0.01$ as compared with sham values). OPG-treated sarcoma-injected animals did not show any SPR internalization (0 ± 0 SPR-IR endosomes/L4 section; $P < 0.01$ *versus* day 21 vehicle-treated sarcoma-injected animals; $P < 0.001$ *versus* day 12 sarcoma-injected animals).

OPG treatment did not affect the mean weight for day 21 vehicle-treated sarcoma-injected animals (22.1 ± 0.9 g), day 21 OPG-treated sarcoma-injected animals (20.4 ± 0.6 g), and sham-injected animals (19.7 ± 1.5 g).

DISCUSSION

The Mouse Model Mirrors Advanced Lytic Bone Cancer in Humans. The mouse model used appears to mirror the tumor-induced bone destruction and tumor-induced pain observed in patients with lytic bone cancer. Histological evidence of initial bone destruction was observed 6 days after injection of the osteolytic 2472 sarcoma cell line into the intramedullary space of the murine femur, and bone destruction continued to progress so that by 12 days after injection of the lytic tumor cells, advanced bone destruction was radiologically evident. By 21 days after injection, fracture of the distal femur was frequently present. The pattern of bone destruction in the model can be described as having a moth-eaten appearance on the endosteal surface of both the distal and proximal regions of the femur, similar to that commonly observed in humans with osteosarcoma (42, 43). Histologically, tumor presence in the intramedullary space and an increase in the number of activated osteoclasts are also evident in the murine model and in humans (16, 44). Thus, radiological and histological features of the murine model of advanced bone cancer are similar to what is observed clinically in humans with advanced bone cancer.

Pain is the most frequent symptom of primary bone cancer and/or bony metastasis (1, 2, 4, 5). Significant ongoing pain is the major impetus for individuals to see a physician. Thus, particularly in the case of relapse, patients frequently present when significant bone destruction has already occurred (1, 2, 5, 21). In patients with bone cancer, the associated pain can be divided into ongoing and breakthrough pain (7–9, 45–47). In the murine model of bone cancer pain, tumor-bearing animals also exhibited ongoing pain and pain exacerbated by movement, thus mirroring humans with bone cancer pain. In the mouse model, ongoing pain was measured by quantifying the number of spontaneous flinches when the animal is at rest. Limb use score, activity-related guarding, and palpation-evoked flinching were measured to assess movement-evoked pain. These behaviors positively correlate with tumor-induced bone destruction (30). Importantly, from the standpoint of assessing the behavior using this model, there is no significant deterioration of the general health of the animal as determined by luster of the coat, appetite, weight loss, or general appearance because in this model, bone cancer pain is limited to one femur.

OPG Administration Rapidly Halts Further Bone Destruction when Treatment Is Initiated after Extensive Intramedullary Tumor Growth and Bone Destruction Has Occurred. Normal bone is constantly being remodeled by osteoclasts that resorb bone and osteoblasts that form bone. Bone resorption and formation are usually tightly controlled so that one does not predominate over the other (48). However, pathological states can disrupt the homeostatic mechanisms that control bone resorption and formation. On their cell surface, stromal cells, osteoblasts, and activated T-lymphocytes express a protein that is a member of the TNF ligand superfamily called RANKL (49, 50). RANKL is also known as TNF-related activation-induced cytokine, osteoclast differentiation factor, or OPGL (49–52). This molecule interacts with a cell membrane protein of the TNF receptor superfamily expressed by preosteoclasts, which is called RANK (53). The crucial roles of RANKL and RANK are demonstrated by the observations that mice with targeted deletions for either of these molecules have no osteoclasts and develop osteopetrosis (54, 55). Thus, osteoclast activation requires the interaction of the RANK receptor located on osteoclast precursor cells with RANKL or OPGL expressed on osteoblasts (53, 56). An increase in the RANK-RANKL (OPGL) interaction, which in turn drives excessive osteoclast activity, is a result of factors released from the tumor/and or bone (20, 48, 54, 57). OPG, a naturally secreted protein, is also a member of the TNF receptor superfamily and thus can bind RANKL with high affinity. However, OPG lacks a transmembrane-spanning domain and therefore cannot couple to intracellular processes (58). Thus, OPG is a soluble "decoy" receptor that, based on its ability to prevent the RANK-RANKL interaction, can prevent osteoclastogenesis.

In mice at day 12 after injection of sarcoma cells, significant bone destruction was evident. Administration of OPG rapidly halts further tumor-induced bone destruction. Previous studies in cell culture and in C3H mice have shown that OPG induces osteoclast apoptosis within 48 h of administration (59). In the present study, bone destruction scores of tumor-injected femora were rapidly stabilized after OPG administration. This suggests that even after extensive tumor-induced bone destruction has occurred, ongoing osteoclast activity is essential for further bone destruction to occur.

In patients with bone cancer, aside from pain, loss of mobility due to tumor-induced mechanical weakening and ultimate fracture of the bone is the event that has the greatest impact on reducing the patients' quality of life (60). The ability to block tumor-induced bone destruction with OPG, even once significant bone destruction has occurred, opens up the possibility of therapeutic interventions that would increase bone formation and mechanically strengthen the bone. The intervention would thereby improve mobility as well as reduce the likelihood of fracture (61). In the present study, sham and tumor-injected mice treated with OPG did not show a significant increase in bone mass, even though bone resorption had been halted. However, mice were only examined from days 12–21 (9 days) after tumor implantation, a time period that may not be sufficient to deduce long-term effects of OPG on bone mass. Humans with bone cancer often have a longer course of treatment (years instead of weeks), thereby presenting the opportunity for an increase in bone mass. If bone formation can be stimulated in the presence of OPG, there is the potential to rebuild bone destroyed by tumor-induced osteoclastic activity. Administration of parathyroid hormone has been shown to induce bone formation (62–66). If parathyroid hormone were given in combination with OPG, there is the potential to restore the structural integrity of the bone. Blocking ongoing bone resorption while enhancing bone formation is a therapeutically relevant mechanism that could potentially improve the structural integrity of affected bones, prevent fractures, enhance mobility, and, ultimately, improve the overall quality of life of cancer patients.

OPG Treatment Reduces Ongoing and Movement-evoked Pain-related Behaviors in Mice with Advanced Bone Cancer. In the present study, even when advanced bone destruction had already occurred, both ongoing and movement-evoked pain did not further escalate once OPG treatment was initiated. These findings suggest that ongoing osteoclast activity, as reflected by bone destruction, plays a significant role in the generation and maintenance of advanced bone cancer pain. There are several mechanisms by which osteoclasts may be involved in generating and maintaining bone cancer pain. For osteoclasts to resorb bone, they must maintain an acidic pH (pH 4.0–5.0) microenvironment at the osteoclast-mineralized bone inter-

face (67). A population of sensory neurons that innervate bone expresses acid-sensing ion channels and vanilloid receptors (68). These neurons could be excited and/or sensitized if exposed to the acidic extracellular microenvironment of the osteoclasts. Also, sensory neurons have been shown to be excited and/or sensitized by growth factors (35, 69–73). A variety of growth factors that reside in bone are released during cancer-induced bone resorption (20, 74, 75). Additionally, as the tumor continues to induce excessive osteoclast-mediated bone resorption, the bone is weakened over time, becomes mechanically compromised, and, ultimately, will fracture. As the bone weakens, mechanical stress on the bone would be expected to place the bone under torsion, which would excite the mechanosensitive fibers present in the richly innervated periosteum, resulting in significant movement-evoked pain.

Whereas OPG clearly reduces advanced bone cancer-related pain, there is also a component of the bone cancer pain that continues despite nearly complete inhibition of osteoclast-mediated bone resorption. A key question in designing novel strategies to effectively block bone cancer pain is to identify the mechanisms by which this residual pain is generated and maintained. Previous studies have suggested that there is relatively little direct sensory and sympathetic innervation of tumors (76). However, malignant cells are known to secrete prostaglandins, endothelins, cytokines, epidermal growth factor, transforming growth factor, and platelet-derived growth factor, and many of these factors have been shown to excite primary afferent nociceptors and thus may be involved in driving a component of non-osteoclast-mediated bone cancer pain (20, 75, 77–82). Inflammation and the tumor environment may also lead to an up-regulation of receptors and enzymes that may serve to contribute to changes in the local microenvironment, leading to changes in the response properties of primary afferent neurons innervating the affected bone. Identifying which factors are involved in this non-osteoclast-mediated pain may not only result in novel non-opiate therapies for treating bone cancer pain but may also shed light on the factors that contribute to the generation and maintenance of cancer pain originating from soft tumors.

Eliminating Osteoclast Activity Reduces Tumor-induced Neurochemical Reorganization of the Spinal Cord and Primary Afferent Sensitization. One of the most important concepts to emerge in the past decade has been that the biochemical and physiological status of the sensory neuron and spinal cord change dynamically to reflect the integrity and status of the innervated tissue. Each neuron in the nociceptive pathway has the capacity to change phenotype in the face of a sustained peripheral injury (83). There is growing evidence to indicate that the role of particular neuronal subsystems in nociception may only become apparent during the process of injury and repair. In the present study, this plasticity is clearly evident because tumor cells proliferate and induce bone destruction so that by day 12, when significant bone destruction was radiologically evident, a significant sensitization of primary afferent neurons and a neurochemical reorganization were also apparent.

In animal models of chronic pain, the two most well-documented mechanisms involved in the dynamic changes contributing to the generation and maintenance of chronic pain are peripheral and central sensitization (84). Sensitization refers to an enhanced response to a noxious stimulation (hyperalgesia) or an inappropriate pain sensation to innocuous stimuli, such as touch and pressure (allodynia). This sensitization can be described as either peripheral or central (the former refers to changes that take place in the primary afferent neuron, whereas central sensitization refers to changes that have occurred in the spinal cord or brain).

In the present model, at 12 days after tumor implantation, primary afferent sensitization with accompanying hyperalgesia and allodynia is already evident with behavioral and neurochemical approaches. In previous reports, SPR internalization and accompanying expression of c-Fos have been used as markers of activation of nociceptive primary afferent neurons (16, 23, 27–29, 85–87). SPR internalization has been used to image the release of substance P from primary afferent neurons after nociceptive stimuli (28, 29). Similarly, c-Fos immunoreactivity has been used to identify neurons responding to painful stimuli (23). Thus, in either naïve or sham-operated animals that received saline injection into the femur, normally non-noxious palpation does not induce SPR internalization or expression of c-Fos in lamina I neurons. However, in tumor-bearing animals, a normally non-noxious palpation of the femur induces SPR internalization and c-Fos expression in lamina I spinal neurons, and both of these changes correlate with the extent of bone destruction and pain-related behaviors.

Similarly, at 12 days after tumor implantation, central sensitization also appears to be present in the model of bone cancer pain. Thus, in ipsilateral spinal cord segments that receive primary afferent input from the cancerous femur, we detected several notable neurochemical changes that peaked at lumbar level L4, the major termination site of sensory fibers that innervate the femur (32). These neurochemical changes have been observed in other chronic pain states and include an increase in the expression of the prohyperalgesic peptide DYN in the deep dorsal horn, an increase in the basal number of immediate early gene protein product c-Fos-positive neurons located in the deep dorsal horn, and a massive hypertrophy of astrocytes (87).

Of particular significance in these studies, we demonstrate that OPG treatment begun at day 12 after implantation of tumor cells, when significant bone destruction and cancer pain are already evident, leads to a significant reduction in spinal neurochemical markers of peripheral and central sensitization. Thus, after OPG treatment, palpation-induced SPR internalization and c-Fos expression in lamina I neurons in sarcoma-bearing animals are reduced, suggesting that tumor-induced peripheral sensitization of primary afferent neurons is significantly blunted. Likewise, OPG treatment reduces the up-regulation of the prohyperalgesic peptide DYN in the spinal cord as well as that of c-Fos in the deep dorsal horn that is otherwise observed in the sarcoma-bearing animals.

What is most impressive about these results is not only the extent and how rapidly these neurochemical changes are induced in a chronic pain state but also how quickly these changes are reversed when the pain is reduced. Thus, although OPG treatment was maintained for only 9 days, from days 12–21, OPG administration was effective at reducing markers of both peripheral and central sensitization, suggesting that ongoing osteoclast activity is required for the full development of both peripheral sensitization and central sensitization that occurs in bone cancer pain.

Summary. The mouse model of bone cancer pain shares many features with advanced bone cancer pain encountered in humans. Thus, animals with sarcoma showed bone destruction, pain-related behaviors, sensitization of primary afferent fibers, and central sensitization with an accompanying neurochemical reorganization of the spinal cord. Osteoclasts clearly play a role in the generation and maintenance of advanced bone cancer pain, and therapies aimed at reducing or blocking osteoclast function may play a useful therapeutic role in reducing pain in patients with advanced bone cancer pain. Whereas osteoclastic activity is pivotal, factors other than osteoclasts are also clearly involved in generating and maintaining a component of bone cancer pain. Ongoing studies using the mouse model of bone cancer pain should permit further definition of the basic mechanisms involved in the generation and maintenance of advanced bone cancer pain. Such mechanistic insights will likely be important in the development of novel therapies for treating bone cancer pain.

ACKNOWLEDGMENTS

We thank Drs. James D. Pomonis (Minneapolis, MN) and Tony L. Yaksh (University of California San Diego, San Diego, CA) for critical review of the manuscript and Dr. David L. Lacey (Amgen, Thousand Oaks, CA) for the gift of OPG.

REFERENCES

1. Rosier, R. Bone pain. Am. J. Hospice Palliative Care, *9:* 37, 1992.
2. Lipton, A. Bisphosphonates and breast carcinoma. Cancer (Phila.), *80:* 1668–1673, 1997.
3. Mercadante, S. Malignant bone pain: pathophysiology and treatment. Pain, *69:* 1–18, 1997.
4. Fulfaro, F., Casuccio, A., Ticozzi, C., and Ripamonti, C. The role of bisphosphonates in the treatment of painful metastatic bone disease: a review of Phase III trials. Pain, *78:* 157–169, 1998.
5. Pecherstorfer, M., and Vesely, M. Diagnosis and monitoring of bone metastases: clinical means. *In:* J-J. Body (ed.), Tumor Bone Diseases and Osteoporosis in Cancer Patients, pp. 97–129. New York: Marcel Dekker, Inc., 2000.
6. Portenoy, R. K., and Hagen, N. A. Breakthrough pain: definition, prevalence and characteristics. Pain, *41:* 273–281, 1990.
7. Mercadante, S., and Arcuri, E. Breakthrough pain in cancer patients: pathophysiology and treatment. Cancer Treat. Rev., *24:* 425–432, 1998.
8. Portenoy, R. K., Payne, D., and Jacobsen, P. Breakthrough pain: characteristics and impact in patients with cancer pain. Pain, *81:* 129–134, 1999.
9. Cherny, N. I., and Portenoy, R. K. The management of cancer pain. CA Cancer J. Clin., *44:* 263–303, 1994.
10. Portenoy, R. K. Pharmacologic management of cancer pain. Semin. Oncol., *22:* 112–120, 1995.
11. Cherny, N. I. The management of cancer pain. CA Cancer J. Clin., *50:* 70–116; quiz, 117–20, 2000.
12. Hoskin, P. J. Radiotherapy in symptom management. *In:* D. Doyle, G. W. Hanks, and N. MacDonald (eds.), Oxford Textbook of Palliative Medicine, pp. 117–129. Oxford, United Kingdom: Oxford Medical Publications, 1993.
13. Hoskin, P. J. Radiotherapy for bone pain. Pain, *63:* 137–139, 1995.
14. Coyle, N., Adelhardt, J., Foley, K. M., and Portenoy, R. K. Character of terminal illness in the advanced cancer patient: pain and other symptoms during the last four weeks of life. J. Pain Symptom Management, *5:* 83–93, 1990.
15. Clohisy, D. R., Ogilvie, C. M., Carpenter, R. J., and Ramnaraine, M. L. Localized, tumor-associated osteolysis involves the recruitment and activation of osteoclasts. J. Orthop. Res., *14:* 2–6, 1996.
16. Honore, P., Luger, N., Sabino, M., Schwei, M., Rogers, S., Mach, D., O'Keefe, P., Ramnaraine, M., Clohisy, D., and Mantyh, P. Osteoprotegerin blocks bone cancer-induced skeletal destruction, skeletal pain and pain-related neurochemical reorganization of the spinal cord. Nat. Med., *6:* 521–528, 2000.
17. Thurlimann, B., and Stoutz, N. D. Causes and treatment of bone pain of malignant origin. Drugs, *51:* 383–398, 1996.
18. Yin, J. J., Selander, K., Chirgwin, J. M., Dallas, M., Grubbs, B. G., Wieser, R., Massague, J., Mundy, G. R., and Guise, T. A. TGF-β signaling blockade inhibits PTHrP secretion by breast cancer cells and bone metastases development. J. Clin. Investig., *103:* 197–206, 1999.
19. Rodan, G., and Martin, T. Therapeutic approaches to bone disease. Science (Wash. DC), *289:* 1508–1514, 2000.
20. Guise, T. A. Molecular mechanisms of osteolytic bone metastases. Cancer (Phila.), *88:* 2892–2898, 2000.
21. Mahan, J., and Seligson, D. Orthopedic management of skeletal metastases. *In:* W. Donegan and J. Spratt (eds.), Cancer of the Breast, 4th ed., pp. 682–695. Philadelphia: W. B. Saunders, 1995.
22. Morony, S., Capparelli, C., Lee, R., Shimamoto, G., Boone, T., Lacey, D. L., and Dunstan, C. R. A chimeric form of osteoprotegerin inhibits hypercalcemia and bone resorption induced by IL-1β, TFN-α, PTH, PTHrP, and 1,25(OH)(2)D_3. J. Bone Miner. Res., *14:* 1478–1485, 1999.
23. Hunt, S. P., Pini, A., and Evan, G. Induction of c-*fos*-like protein in spinal cord neurons following sensory stimulation. Nature (Lond.), *328:* 632–634, 1987.
24. Honore, P., Chapman, V., Buritova, J., and Besson, J. M. To what extent do spinal interactions between an α-2 adrenoceptor agonist and a μ opioid agonist influence noxiously evoked c-Fos expression in the rat? A pharmacological study. J. Pharmacol. Exp. Ther., *278:* 393–403, 1996.
25. Mantyh, P. W., Allen, C. J., Ghilardi, J. R., Rogers, S. D., Mantyh, C. R., Liu, H., Basbaum, A. I., Vigna, S. R., and Maggio, J. E. Rapid endocytosis of a G protein-coupled receptor: substance P evoked internalization of its receptor in the rat striatum *in vivo*. Proc. Natl. Acad. Sci. USA, *92:* 2622–2626, 1995.
26. Abbadie, C., Trafton, J., Liu, H., Mantyh, P. W., and Basbaum, A. I. Inflammation increases the distribution of dorsal horn neurons that internalize the neurokinin-1 receptor in response to noxious and non-noxious stimulation. J. Neurosci., *17:* 8049–8060, 1997.
27. Honore, P., Menning, P. M., Rogers, S. D., Nichols, M. L., Basbaum, A. I., Besson, J-M., and Mantyh, P. W. Spinal substance P receptor expression and internalization in acute, short-term, and long-term inflammatory pain states. J. Neurosci., *19:* 7670–7678, 1999.
28. Mantyh, P. W., Demaster, E., Malhotra, A., Ghilardi, J. R., Rogers, S. D., Mantyh, C. R., Liu, H. T., Basbaum, A. I., Vigna, S. R., Maggio, J. E., and Simone, D. A. Receptor endocytosis and dendrite reshaping in spinal neurons after somatosensory stimulation. Science (Wash. DC), *268:* 1629–1632, 1995.
29. Allen, B. J., Rogers, S. D., Ghilardi, J. R., Menning, P. M., Kuskowski, M. A., Basbaum, A. I., Simone, D. A., and Mantyh, P. W. Noxious cutaneous thermal stimuli induce a graded release of endogenous substance P in the spinal cord-imaging peptide action *in vivo*. J. Neurosci., *17:* 5921–5927, 1997.
30. Schwei, M. J., Honore, P., Rogers, S. D., Johnson, J. L., Finke, M. P., Rarmaraine, M., Clohisy, D. R., and Mantyh, P. W. Neurochemical and cellular reorganization of the spinal cord in a murine model of bone cancer pain. J. Neurosci., *19:* 10886–10897, 1999.
31. Nichols, M. L., Allen, B. J., Rogers, S. D., Ghilardi, J. R., Honore, P., Luger, N. M., Finke, M. P., Li, J., Lappi, D. A., Simone, D. A., and Mantyh, P. W. Transmission of chronic nociception by spinal neurons expressing the substance P receptor. Science (Wash. DC), *286:* 1558–1561, 1999.
32. Molander, C., Xu, Q., and Grant, G. The cytoarchitectonic organization of the spinal cord in the rat. I. The lower thoracic and lumbosacral cord. J. Comp. Neurol., *230:* 133–141, 1984.
33. Bjurholm, A., Kreicbergs, A., Brodin, E., and Schultzberg, M. Substance P- and CGRP-immunoreactive nerves in bone. Peptides, *9:* 165–171, 1988.
34. Hill, E. L., and Elde, R. Distribution of CGRP-, VIP-, DβH-, SP-, and NPY-immunoreactive nerves in the periosteum of the rat. Cell Tissue Res., *264:* 469–480, 1991.
35. Woolf, C. J., Allchorne, A., Safieh-Garabedian, B., and Poole, S. Cytokines, nerve growth factor and inflammatory hyperalgesia: the contribution of tumour necrosis factor α. Br. J. Pharmacol., *121:* 417–424, 1997.
36. Colburn, R. W., Rickman, A. J., and DeLeo, J. A. The effect of site and type of nerve injury on spinal glial activation and neuropathic pain behavior. Exp. Neurol., *157:* 289–304, 1999.
37. Catheline, G., Le Guen, S., Honore, P., and Besson, J. M. Are there long-term changes in the basal or evoked Fos expression in the dorsal horn of the spinal cord of the mononeuropathic rat? Pain, *80:* 347–357, 1999.
38. Hoffman, G., Smith, M. S., and Verbalis, J. cFos and related immediate early gene products as markers of activity in neuroendocrine systems. Front. Neuroendocrinol., *14:* 173–213, 1993.
39. Sagar, S. M., Sharp, F. R., and Curran, T. Expression of c-*fos* protein in brain: metabolic mapping at the cellular level. Science (Wash. DC), *240:* 1328–1331, 1988.
40. Bian, D., Ossipov, M. H., Ibrahim, M., Raffa, R. B., Tallarida, R. J., Malan, T. P., Jr., Lai, J., and Porreca, F. Loss of antiallodynic and antinociceptive spinal/supraspinal morphine synergy in nerve-injured rats: restoration by MK-801 or dynorphin antiserum. Brain Res., *831:* 55–63, 1999.
41. Malan, T. P., Ossipov, M. H., Gardell, L. R., Ibrahim, M., Bian, D., Lai, J., and Porreca, F. Extraterritorial neuropathic pain correlates with multisegmental elevation of spinal dynorphin in nerve-injured rats. Pain, *86:* 185–194, 2000.
42. Bloem and Kroon osseous lesions. The Radiologic Clinics of North America, Vol. 32, pp. 265–278. Philadelphia: W. B. Saunders, 1993.
43. Parsa, M., and Murphey, M. Radiographic diagnosis and monitoring of bone metastases. *In:* J-J. Body (ed.), Tumor Bone Disease and Osteoporosis in Cancer Patients, pp. 155–195. New York: Marcel Dekker, Inc., 2000.
44. Taube, T., Elomaa, I., Blomqvist, C., Beneton, M. N., and Kanis, J. A. Histomorphometric evidence for osteoclast-mediated bone resorption in metastatic breast cancer. Bone, *15:* 161–166, 1994.
45. Payne, R. Mechanisms and management of bone pain. Cancer (Phila.), *80:* 1608–1613, 1997.
46. Portenoy, R. K., and Lesage, P. Management of cancer pain. Lancet, *353:* 1695–1700, 1999.
47. Foley, K. M. Advances in cancer pain. Arch. Neurol., *56:* 413–417, 1999.
48. Teitelbaum, S. L. Bone resorption by osteoclasts. Science (Wash. DC), *289:* 1504–1508, 2000.
49. Anderson, D. M., Maraskovsky, E., Billingsley, W. L., Dougall, W. C., Tometsko, M. E., Roux, E. R., Teepe, M. C., DuBose, R. F., Cosman, D., and Galibert, L. A homologue of the TNF receptor and its ligand enhance T-cell growth and dendritic-cell function. Nature (Lond.), *390:* 175–179, 1997.
50. Yasuda, H., Shima, N., Nakagawa, N., Yamaguchi, K., Kinosaki, M., Mochizuki, S., Tomoyasu, A., Yano, K., Goto, M., Murakami, A., Tsuda, E., Morinaga, T., Higashio, K., Udagawa, N., Takahashi, N., and Suda, T. Osteoclast differentiation factor is a ligand for osteoprotegerin/osteoclastogenesis-inhibitory factor and is identical to TRANCE/RANKL. Proc. Natl. Acad. Sci. USA, *95:* 3597–3602, 1998.
51. Wong, B. R., Rho, J., Arron, J., Robinson, E., Orlinck, J., Chao, M., Kalachikov, S., Cayani, E., Barlett, F. S., III, Frankel, W. N., Lee, S. Y., and Choi, Y. TRANCE is a novel ligand of the tumor necrosis factor receptor family that activates c-Jun N-terminal kinase in T cells. J. Biol. Chem., *272:* 25190–25194, 1997.
52. Lacey, D. L., Timms, E., Tan, H. L., Kelley, M. J., Dunstan, C. R., Burgess, T., Elliott, R., Colombero, A., Elliott, G., Scully, S., Hsu, H., Sullivan, J., Hawkins, N., Davy, E., Capparelli, C., Eli, A., Qian, Y. X., Kaufman, S., Sarosi, I., Shalhoub, V., Senaldi, G., Guo, J., Delaney, J., and Boyle, W. J. Osteoprogegerin ligand is a cytokine that regulates osteoclast differentiation and activation. Cell, *93:* 165–176, 1998.
53. Hsu, H., Lacey, D. L., Dunstan, C. R., Solovyev, I., Colombero, A., Timms, E., Tan, H. L., Elliott, G., Kelley, M. J., Sarosi, I., Wang, L., Xia, X. Z., Elliott, R., Chiu, L., Black, T., Scully, S., Capparelli, C., Morony, S., Shimamoto, G., Bass, M. B., and Boyle, W. J. Tumor necrosis factor receptor family member RANK mediates osteoclast differentiation and activation induced by osteoprotegerin ligand. Proc. Natl. Acad. Sci. USA, *96:* 3540–3545, 1999.
54. Kong, Y. Y., Yoshida, H., Sarosi, I., Tan, H. L., Timms, E., Capparelli, C., Morony, S., Oliveira-dos-Santos, A. J., Van, G., Itie, A., Khoo, W., Wakeham, A., Dunstan, C. R., Lacey, D. L., Mak, T. W., Boyle, W. J., and Penninger, J. M. OPGL is a key regulator of osteoclastogenesis, lymphocyte development and lymph-node organogenesis. Nature (Lond.), *397:* 315–323, 1999.

55. Li, J., Sarosi, I., Yan, X. Q., Morony, S., Capparelli, C., Tan, H. L., McCabe, S., Elliott, R., Scully, S., Van, G., Kaufman, S., Juan, S. C., Sun, Y., Tarpley, J., Martin, L., Christensen, K., McCabe, J., Kostenuik, P., Hsu, H., Fletcher, R., Dunstan, C. R., Lacey, D. L., and Boyle, W. J. RANK is the intrinsic hematopoietic cell surface receptor that osteoclastogenesis and regulation of bone mass and calcium metabolism. Proc. Natl. Acad. Sci. USA, *97:* 1566–1571, 2000.
56. Takayanagi, H., Ogasawara, K., Hida, S., Chiba, T., Murata, S., Sato, K., Takaoka, A., Yokochi, T., Oda, H., Tanaka, K., Nakamura, K., and Taniguchi, T. T-cell-mediated regulation of osteoclastogenesis by signaling cross-talk between RANKL and IGN-γ. Nature (Lond.), *408:* 600–605, 2000.
57. Lacey, D. L., Timms, E., Tan, H. L., Kelley, M. J., Dunstan, C. R., Burgess, T., Elliott, R., Colombero, A., Elliott, G., Scully, S., Hsu, H., Sullivan, J., Hawkins, N., Davy, E., Capparelli, C., Eli, A., Qian, Y. X., Kaufman, S., Sarosi, I., Shalhoub, V., Senaldi, G., Guo, J., Delaney, J., and Boyle, W. J. Osteoprotegerin ligand is a cytokine that regulates osteoclast differentiation and activation. Cell, *93:* 165–176, 1998.
58. Simonet, W. S., Lacey, D. L., Dunstan, C. R., Kelley, M., Chang, M. S., Luthy, R., Nguyen, H. Q., Wooden, S., Bennett, L., Boone, T., Shimamoto, G., Derose, M., Elliott, R., Colombero, A., Tan, H. L., Trail, G., Sullivan, J., Davy, E., Bucay, N., Renshawgegg, L., Hughes, T. M., Hill, D., Pattison, W., Campbell, P., Sander, S., *et al.* Osteoprotegerin: a novel secreted protein involved in the regulation of bone density. Cell, *89:* 309–319, 1997.
59. Lacey, D., Tan, H., Lu, J., Kaufman, S., Van, G., Qui, W., Rattan, A., Scully, S., Fletcher, F., Juan, T., Kelley, M., Burgess, T., Boyle, W., and Polverino, A. Osteoprotegerin ligand modulates murine osteoclast survival *in vitro* and *in vivo.* Am. J. Pathol., *157:* 435–448, 2000.
60. Coleman, R. E. Skeletal complications of malignancy. Cancer (Phila.), *80:* 1588–1594, 1997.
61. Rodan, G. A., and Martin, T. J. Therapeutic approaches to bone diseases. Science (Wash. DC), *289:* 1508–1514, 2000.
62. Dempster, D., Cosman, F., Parisien, M., Shen, V., and Lindsay, R. Anabolic actions of parathyroid hormone on bone. Endoc. Rev., *14:* 690–709, 1993.
63. Reeve, J. PTH: a future role in the management of osteoporosis? J. Bone Miner. Res., *11:* 440–445, 1996.
64. Lindsay, R., Nieves, J., Formica, C., Henneman, E., Woelfert, L., Shen, V., Dempster, D., and Cosman, F. Randomised controlled study of effect of parathyroid hormone on vertebral-bone mass and fracture incidence among postmenopausal women on oestrogen with osteoporosis. Lancet, *350:* 550–555, 1997.
65. Morley, P., Whitfield, J., and Willick, G. Anabolic effects of parathyroid hormone on bone. Trends Endocrinol. Metab., *8:* 225–231, 1997.
66. Jilka, R. L., Weinstein, R. S., Bellido, T., Roberson, P., Parfitt, A. M., and Manolagas, S. C. Increased bone formation by prevention of osteoblast apoptosis with parathyroid hormone. J. Clin. Investig., *104:* 439–446, 1999.
67. Delaisse, J-M., and Vaes, G. Mechanism of mineral solubilization and matrix degradation in osteoclastic bone resorption. *In:* B. R. Rifkin and C. V. Gay (eds.), Biology and Physiology of the Osteoclast, pp. 289–314. Ann Arbor, MI: CRC-Press, 1992.
68. Olson, T. H., Riedl, M. S., Vulchanova, L., Ortiz-Gonzalez, X. R., and Elde, R. An acid sensing ion channel (ASIC) localizes to small primary afferent neurons in rats. Neuroreport, *9:* 1109–1113, 1998.
69. Hauschka, P. V., Mavrakos, A. E., Iafrati, M. D., Doleman, S. E., and Klagsbrun, M. Growth factors in bone matrix. Isolation of multiple types by affinity chromatography on heparin-Sepharose. J. Biol. Chem., *261:* 12665–12674, 1986.
70. Pfeilschifter, J., and Mundy, G. R. Modulation of type β transforming growth factor activity in bone cultures by osteotropic hormones. Proc. Natl. Acad. Sci. USA, *84:* 2024–2028, 1987.
71. Watkins, L. R., Wiertelak, E. P., Goehler, L. E., Smith, K. P., Martin, D., and Maier, S. F. Characterization of cytokine-induced hyperalgesia. Brain Res., *654:* 15–26, 1994.
72. Safieh-Garabedian, B., Poole, S., Allchorne, A., Winter, J., and Woolf, C. J. Contribution of interleukin-1 β to the inflammation-induced increase in nerve growth factor levels and inflammatory hyperalgesia. Br. J. Pharmacol., *115:* 1265–1275, 1995.
73. Sorkin, L. S., Xiao, W. H., Wagner, R., and Myers, R. R. Tumour necrosis factor-α induces ectopic activity in nociceptive primary afferent fibres. Neuroscience, *81:* 255–262, 1997.
74. Goni, M. H., and Tolis, G. Hypercalcemia of cancer: an update. Anticancer Res., *13:* 1155–1160, 1993.
75. Suzuki, K., and Yamada, S. Ascites sarcoma 180, a tumor associated with hypercalcemia, secretes potent bone-resorbing factors including transforming growth factor interleukin-1 α and interleukin-6. Bone Min., *27:* 219–233, 1994.
76. O'Connell, J. X., Nanthakumar, S. S., Nielsen, G. P., and Rosenberg, A. E. Osteoid osteoma: the uniquely innervated bone tumor. Mod. Pathol., *11:* 175–180, 1998.
77. Kusuhara, M., Yamaguchi, K., Nagasaki, K., Hayashi, C., Suzaki, A., Hori, S., Handa, S., Nakamura, Y., and Abe, K. Production of endothelin in human cancer cell lines. Cancer Res., *50:* 3257–3261, 1990.
78. Oikawa, T., Kushuhara, M., Ishikawa, S., Hitomi, J., Kono, A., Iwanaga, T., and Yamaguchi, K. Production of endothelin-1 and thrombomodulin by human pancreatic cancer cells. Br. J. Cancer, *69:* 1059–1064, 1994.
79. Nelson, J. B., Hedican, S. P., George, D. J., Reddi, A. H., Piantadosi, S., Eisenberger, M. A., and Simons, J. W. Identification of endothelin-1 in the pathophysiology of metastatic adenocarcinoma of the prostate. Nat. Med., *1:* 944–949, 1995.
80. Pekonen, F., Nyman, T., Ammala, M., and Rutanen, E. M. Decreased expression of messenger RNAs encoding endothelin receptors and neutral endopeptidase 24.11 in endometrial cancer. Br. J. Cancer, *71:* 59–63, 1995.
81. Sulzbacher, I., Traxler, M., Mosberger, I., Lang, S., and Chott, A. Platelet-derived growth factor-AA and α receptor expression suggests an autocrine and/or paracrine loop in osteosarcoma. Mod. Path., *13:* 632–637, 2000.
82. Liang, G., Robertson, K. D., Talmadge, C., Sumegi, J., and Jones, P. A. The gene for a novel transmembrane protein containing epidermal growth factor and follistatin domains is frequently hypermethylated in human tumor cells. Cancer Res., *60:* 4907–4912, 2000.
83. Woolf, C. J., and Salter, M. W. Neuronal plasticity: increasing the gain in pain. Science (Wash. DC), *288:* 1765–1769, 2000.
84. Ma, Q. P., and Woolf, C. J. Progressive tactile hypersensitivity: an inflammation-induced incremental increase in the excitability of the spinal cord. Pain, *67:* 97–106, 1996.
85. Mantyh, P. W., Rogers, S. D., Honore, P., Allen, B. J., Ghilardi, J. R., Li, J., Daughters, R. S., Lappi, D. A., Wiley, R. G., and Simone, D. A. Inhibition of hyperalgesia by ablation of lamina I spinal neurons expressing the substance P receptor. Science (Wash. DC), *278:* 275–279, 1997.
86. Doyle, C. A., and Hunt, S. P. Substance P receptor (neurokinin-1)-expressing neurons in lamina I of the spinal cord encode for the intensity of noxious stimulation: a c-Fos study in rat. Neuroscience, *89:* 17–28, 1999.
87. Honore, P., Rogers, S. D., Schwei, M. J., Salak-Johnson, J. L., Luger, N. M., Sabino, M. C., Clohisy, D. R., and Mantyh, P. W. Murine models of inflammatory, neuropathic and cancer pain each generates a unique set of neurochemical changes in the spinal cord and sensory neurons. Neuroscience, *98:* 585–598, 2000.